EUROPEAN ORGANIZATION FOR NUCLEAR RESEARCH

CERN-PPE/97-43
25 April 1997

Production of e, μ and τ Pairs in Untagged Two-Photon Collisions at LEP

The L3 Collaboration

Abstract

The two-photon collision reaction $e^+e^- \to e^+e^-l^+l^-$ has been studied at $\sqrt{s} \approx 91$ GeV using the L3 detector at LEP for $l = e, \mu, \tau$. We have analysed untagged configurations where the two photons are quasi-real. Good agreement is found between our measurements and the $\mathcal{O}(\alpha^4)$ QED expectation.

Submitted to *Phys. Lett. B*

Introduction

The large acceptance and high precision detectors at the LEP collider are well suited for the study of the processes :

$$e^+e^- \to e^+e^- \; l^+ \; l^- \quad (l = e, \mu, \tau) \; .$$

The l^+l^- pair can either be produced in a $C = +1$ state by the collision of two virtual photons (Fig. 1a) or in a $C = -1$ state by the bremsstrahlung of a single virtual photon (Fig. 1b). For untagged events, where the e^+ or e^-, scattered at very small angles, are not observed, the cross section is dominated by the multiperipheral $\gamma\gamma$ collision process shown in Fig. 1a . The observed cross section, allowing for the limited angular acceptance of the detector, increases as $\ln^2 s$ (where s is the square of the centre-of-mass energy). The kinematical separation from the one-boson annihilation process $e^+e^- \to l^+l^-$ also increases with increasing energy. Thus LEP is favoured relative to lower energy colliders [1] for the study of the process $e^+e^- \to e^+e^-l^+l^-$. The cross sections and distributions for these processes provide a test of QED to order α^4 over a wide kinematical range.

In this paper, we present a study of untagged $e^+e^- \to e^+e^-l^+l^-$ events performed with the L3 detector [2]. For e- and μ-pair production the data were taken in 1992 and 1993 at $\sqrt{s} \approx 91$ GeV, corresponding to a total integrated luminosity of 52 pb^{-1}. For τ-pair production, where the statistical limitations are more important, we have also included the 1994 data, obtaining a total integrated luminosity of 112 pb^{-1}. Since the cross section for τ-pair production is much smaller and the backgrounds are more severe, the analysis was limited to the τ-decay modes: ($e\nu\nu$) ($\mu\nu\nu$) and ($\pi^\pm\pi^0\nu$) ($l^\pm\nu\nu$). The reaction $e^+e^- \to e^+e^-\tau^+\tau^-$ was previously observed by OPAL [3] in the $e\mu$ channel using single-tag event topology. The present measurement is the first time that τ-pair production has been observed in untagged two-photon collisions.

The data were collected using a charged-particle trigger [4] with a transverse momentum (p_t) threshold of 150 MeV. This trigger requires at least two charged tracks to be back-to-back in the plane transverse to the beam within $\pm 41°$. τ pairs may also be accepted by an energy trigger which requires a single cluster deposit in the electromagnetic calorimeter greater than ≈ 1 GeV, and small activity elsewhere. The charged particle trigger efficiency is measured to be $(94.8 \pm 0.6)\%$ using independently triggered Bhabha scattering events.

Monte Carlo Simulation

To calculate the efficiencies and backgrounds for the selection criteria and to compare the data to the QED predictions, the generator of Berends, Daverveldt and Kleiss (BDK [5]) is used. The BDK generator calculates the full set of QED diagrams to $\mathcal{O}(\alpha^4)$, taking into account interference effects.

For background studies, such as resonances and pion-pair production, we have used the EGPC [6] Monte Carlo which generates the two-photon process using the exact transverse luminosity function. The decays of hadronic resonances are generated according to phase space. The events were fully simulated in the L3 detector [7], taking into account detector and trigger inefficiencies. They were reconstructed and analysed with the same programs as the data. The charged-particle trigger is also simulated, using the inefficiencies measured in independently triggered Bhabha scattering events.

Event Selection

We initially select events by requiring two well-reconstructed tracks. The track criteria are:

- at least 12 hits in the tracking chamber,
- the distance of closest approach to the interaction point in the transverse plane smaller than 10 mm,
- a transverse momentum greater than 0.1 GeV,
- a corresponding signal in the electromagnetic calorimeter.

The two tracks must also have opposite charge. Events with a scattered electron of energy greater than 35 GeV in the luminosity monitor are rejected. This 'anti-tag' requirement limits the Q^2 of a photon to be less than 1 GeV^2. The total energy in the calorimeters must be less than 60 GeV to remove one-boson annihilation background.

Three Neural Networks (NN) trained to identify separately e, μ and π have been developed for this analysis [8]. For each particle species, a different NN with ten input neurons, a single layer of eleven hidden neurons and one output neuron was used. The following measured quantities are associated with the ten input neurons:

- $E_{\rm t}/p_{\rm t}$, where $E_{\rm t}$ is the transverse energy measured in the electromagnetic calorimeter and $p_{\rm t}$ is the transverse momentum measured in the tracker.
- A χ^2 calculated from the mean specific energy loss dE/dx measured in the tracker. Two χ^2 values are found that test the compatibility of the measured dE/dx with the signal expected from either a minimum ionising particle (MIP) or an electron. The NN input quantity is then the normalized χ^2 probability difference :

$$\frac{P_{\chi^2_e} - P_{\chi^2_{MIP}}}{P_{\chi^2_e} + P_{\chi^2_{MIP}}} \ .$$

- Four quantities related to the electromagnetic shower in the calorimeter: the number of BGO crystals, $S_9,\ S_1/S_2,\ S_1/S_6$, where S_1 is the energy deposited in the central crystal of the electromagnetic cluster and S_n $(n = 2, 6, 9)$ is the energy sum of the n most energetic crystals in the cluster.
- The number of electromagnetic clusters associated with the track.
- Three quantities related to the development of the shower in the hadron calorimeter: the number of hits in the calorimeter, the distance between the first and the last hit and the shower length. All of these are normalized to the expectation for a minimum ionising particle.

Each NN was trained with a sample consisting of electrons, muons and pions from a Monte Carlo simulation of the reaction $e^+e^- \to e^+e^-\tau^+\tau^-$. To optimize the training process, the mean value of each variable, estimated by the Monte Carlo, was subtracted before input to the NN. The NNs are each trained so that the value of the output neuron, ζ, is close to 1.0 for the

desired particle type. The performance of the NN is defined by its efficiency, $\mathcal{E}_i$, and its purity, $\mathcal{P}_i$. For the electron NN, for example, these are defined as:

$$\mathcal{E}_{\rm e} = \frac{N_{\rm ee}}{N_{\rm ee} + N_{\rm ex}} \quad \text{and} \quad \mathcal{P}_{\rm e} = \frac{N_{\rm ee}}{N_{\rm ee} + N_{\rm xe}},$$

where $N_{\rm ee}$ is the number of electrons correctly identified as electrons, $N_{\rm ex}$ the number of misidentified electrons and $N_{\rm xe}$ the number of non-electrons wrongly identified as electrons. The performances of the three NNs with the identification criteria, ζ_e >0.7, ζ_μ >0.7, ζ_π >0.78, are presented in Table 1 for a Monte Carlo sample of 10000 events of the type $\rm e^+e^- \to e^+e^-\tau^+\tau^-$, where ζ_e, ζ_μ, and ζ_π are the outputs of the electron, muon and pion networks, respectively.

Electron and Muon Pair Analyses

The following further cuts are applied to select candidates for e- and μ-pair events [9]:

- The two charged tracks must each be in the polar angle range $44^\circ < \theta < 136^\circ$.
- The square of the total transverse momentum of the lepton pair $(\sum \vec{p_{\rm t}})^2$ must be smaller than 0.02 $\rm GeV^2$ (see Fig. 2). Below 0.02 $\rm GeV^2$ the Monte Carlo reproduces the data well. This cut removes background events of the type $\pi^+\pi^-$X, where X represents one or more unobserved particles, and also lepton-pair events with large photon virtuality.

Electrons are identified by combining information from the tracker and the electromagnetic calorimeter. The energy in the latter is required to be greater than 0.35 GeV, in order to reject minimum ionising particles. Matching is required between the $p_{\rm t}$ and the $E_{\rm t}$, i.e. $E_{\rm t}/p_{\rm t}$ larger than 0.8. Electron-pair candidate events are those in which at least one track satisfies the selection criteria for an electron. We select 30584 events in the mass interval $0.5 \leq M_{\rm ee} \leq 45$ GeV. In 60% of the events, both tracks are identified as electrons.

Muons produced in the two-photon process generally have low momentum and very few reach the muon chambers. So muons are identified by requiring that the signal in the electromagnetic and hadronic calorimeters be consistent with a minimum ionising particle. For the selection of muon-pair events at least one track is identified as a muon. The NN is used to reduce pion background: if a track is not positively identified as an e or μ, but is consistent with a π according to the NN, the event is removed. That is, if ζ_e <0.35, ζ_μ <0.35, ζ_π >0.85, the event is removed from the muon-pair sample. We select 11875 events in the mass interval $0.5 \leq M_{\mu\mu} \leq 45$ GeV. In 45% of the events, both tracks are identified as muons.

The background processes listed in Table 2 have been considered. The background fractions are estimated by a Monte Carlo simulation for each process after applying the event and particle selection cuts described above. The most important background for e-pairs is misidentified μ-pairs (0.85%) and for μ-pairs, it is misidentified π-pairs, dominated by the process: $\rm e^+e^- \to e^+e^- f_2$ ($f_2 \to \pi^+\pi^-$) (3.6%).

For the calculation of acceptance and efficiency, we have generated events with the BDK Monte Carlo in the polar angular range $10^\circ \leq \theta \leq 170^\circ$ with an effective two-photon mass cut $W_{\gamma\gamma} \geq 300$ MeV. For the electron-pair channel we have generated a Monte Carlo sample of 528K events and for the muon pairs a sample of 240K events. The efficiency is defined as:

$$\epsilon \;=\; \frac{N^{\rm acc}_{\rm rec}(44^\circ \leq \theta \leq 136^\circ)}{N_{\rm gen}(44^\circ \leq \theta \leq 136^\circ)}, \qquad (1)$$

where $N_{\rm gen}$ is the number of generated events with $W_{\gamma\gamma} \geq 500$ MeV in the polar angle range between 44° and 136°. $N_{\rm rec}^{\rm acc}$ is the number of reconstructed events passing the cuts described above. The overall efficiency for the electron channel is $(23.0 \pm 0.3)\%$ and for the muon channel $(9.2 \pm 0.2)\%$. For the electrons the main inefficiencies are due to the $(\sum \vec{p}_{\rm t})^2$ and electron energy cuts which reject 20% and 39% of the events respectively. For the muon pairs the $(\sum \vec{p}_{\rm t})^2$ and hadron calorimeter cuts reject 17% and 59% of events respectively.

Tau Pair Analysis

To suppress background, we restrict the τ-pair selection to leptonic τ decays and decays to $\rho\nu$. The following cuts are used [8]:

- The two oppositely charged tracks must each have a momentum between 300 MeV and 10 GeV.
- The acoplanarity angle between the two charged tracks must be greater than 18°. This cut removes background from $\mathrm{e^+e^-} \to \mathrm{e^+e^-}l^+l^-$ (l = e,μ) events which have tracks that are almost back-to-back in the transverse plane.
- For the $\pi^\pm\pi^0\nu$ τ-decay channel, we require two electromagnetic clusters in the polar angle range between 44° and 136° with energy greater than 100 MeV and separated by at least 10° from the nearest charged track. A π^0 signal is seen in the effective mass of the two clusters (see Fig. 3a). We define the π^0 region as $115 < M_{\gamma\gamma} < 155$ MeV.

Tau-pair candidates in the ($e\nu\nu$) ($\mu\nu\nu$) decay mode are identified by the following cuts on the neural network output:

- one track must have $\zeta_e > 0.7$ and the other track must have $\zeta_\mu > 0.7$,
- $(\sum \vec{p}_{\rm t})^2 > 0.5$ GeV^2.

The last cut removes background from misidentified e- and μ-pair events.

Tau-pair candidates in the ($\pi^\pm\pi^0\nu$) ($l\nu\nu$) decay mode are defined by the following selection criteria:

- one track must be identified as a lepton, i.e. $\zeta_e > 0.7$ or $\zeta_\mu > 0.7$,
- one track must be identified as a pion, i.e. neither of the previous conditions is fulfilled,
- the two photons must form a π^0,
- the invariant mass of the $\pi^\pm\pi^0$ must be less than 1.5 GeV, thus imposing a modest ρ mass constraint, see Fig. 3b.
- the invariant mass of the lepton and π^0 must be greater than 0.9 GeV. This cut removes background events from the process : $\mathrm{e^+e^-} \to \mathrm{e^+e^-}\rho^+\rho^-$ ($\rho^\pm \to \pi^\pm\pi^0$) with an unobserved π^0 and a $\pi^\pm$ misidentified as a lepton.

For the eμ channel, the background is dominated by the large cross sections for the processes $\mathrm{e^+e^-}$ and $\mu^+\mu^-$. For the ($l\pi^\pm\pi^0$) channel, the dominant background is hadronic two-photon processes which were simulated using the EGPC generator. To measure the detector and analysis efficiencies, we generated 10000 Monte Carlo events. No mass or angular cut was applied at the generator level. The efficiencies are found to be $(6.8\pm 0.5)\%$ for the eμ channel and $(1.9\pm0.2)\%$ for the $l\pi^\pm\pi^0$ channel.

Results

The observed numbers of events in the different channels are given in Table 3, together with the predictions of the BDK Monte Carlo generator, including the effects of acceptance and trigger efficiency. The first quoted error on the observed number of events is statistical, the second is systematic. The errors quoted on the predictions are the Monte Carlo statistical errors. In all cases, good agreement is found between the data and the BDK predictions.

The data are then corrected for the detection efficiency and normalized to the integrated luminosity, in order to measure cross sections which can be compared with the QED calculations. For the $e^+e^- \to e^+e^-e^+e^-$ and $e^+e^- \to e^+e^-\mu^+\mu^-$ channels, the comparison is given for the angular range ($44^\circ \leq \theta \leq 136^\circ$) and for $W_{\gamma\gamma} \geq 500$ MeV. For the reaction $e^+e^- \to e^+e^-e^+e^-$, we find

$$\sigma_{\rm data} \;=\; 2.56 \pm 0.01\ (\text{stat.}) \pm 0.05\ (\text{syst.})\ \text{nb}$$

to be compared with

$$\sigma_{\rm QED} \;=\; 2.57 \pm 0.02\ (\text{stat.})\ \text{nb}.$$

For the reaction $e^+e^- \to e^+e^-\mu^+\mu^-$, we find

$$\sigma_{\rm data} \;=\; 2.48 \pm 0.02\ (\text{stat.}) \pm 0.06\ (\text{syst.})\ \text{nb}$$

to be compared with

$$\sigma_{\rm QED} \;=\; 2.44 \pm 0.04\ (\text{stat.})\ \text{nb}.$$

To estimate the systematic error due to the selection criteria, we have taken a total of nine different values for each of the cuts around their nominal value. The major source of systematic error, both in the case of the electron and muon, is the $(\sum \vec{p}_{\rm t})^2$ cut. The total systematic error due to the selection criteria is estimated to be 1.7% for electrons and 1.9% for muons. The systematic error due to the background subtraction is estimated to be 0.1% for electrons and 0.4% for muons. The systematic error due to the luminosity measurement is estimated to be 0.6%. The total systematic error on the cross section is thus 2.0% and 2.4% for the electron and the muon channels, respectively.

In Fig. 4a and 4b, we compare the differential cross sections $\mathrm{d}\sigma/\mathrm{d}\Omega$ for the electron pairs and the muon pairs, respectively, to the Monte Carlo predictions as a function of the lepton polar angle in the $\gamma\gamma$ centre-of-mass frame. The agreement is good over the full angular range. In Fig. 5, we compare the invariant mass spectrum of the electron pairs in two-photon collisions for data and Monte Carlo.

For the channel $e^+e^- \to e^+e^-\tau^+\tau^-$ we calculate the total cross section from the two decay channels $e\mu$ and $l\pi^\pm\pi^0$ separately. The τ branching ratios of 6.36% and 18.3% [10] are used respectively for the two channels to calculate the total cross section. The results are

$$\begin{aligned} \sigma_{\rm data} &= 291 \pm 25\ (\text{stat.}) \pm 43\ (\text{syst.})\ \text{pb} && (e\mu\ \text{channel}) \\ \sigma_{\rm data} &= 243 \pm 26\ (\text{stat.}) \pm 31\ (\text{syst.})\ \text{pb} && (l\pi^\pm\pi^0\ \text{channel}) \end{aligned} \tag{2}$$

whereas the combined result from two channels is

$$\sigma_{\rm data} \;=\; 270 \pm 18\ (\text{stat.}) \pm 37\ (\text{syst.})$$

to be compared with

$$\sigma_{\mathrm{QED}} \;=\; 276 \pm 3 \text{ pb}.$$

The effective mass spectra of the measured particles (W_{vis}) are compared with the Monte Carlo predictions for $l\pi^{\pm}\pi^{0}$ (Fig. 6a) and eμ (Fig. 6b) channels. Details of systematic errors are given in Table 4. They include the error on the analysis efficiency and the trigger and background uncertainties. The uncertainty in the neural network selection has been estimated to be $\pm 2\%$ by varying the cuts. The two measured values for the cross sections are consistent with each other within their statistical errors. The systematic error comes mainly from the errors on the particle identification probabilities and from the background subtraction.

The present measurement is the first time that τ-pair production has been observed in untagged two-photon collisions.

Acknowledgments

We wish to express our gratitude to the CERN accelerator divisions for the excellent performance of the LEP machine. We acknowledge the contributions of all the engineers and technicians who have participated in the construction and maintenance of this experiment. Those of us who are not from member states thank CERN for its hospitality and help.

The L3 Collaboration:

M.Acciarri,[28] O.Adriani,[17] M.Aguilar-Benitez,[27] S.Ahlen,[11] J.Alcaraz,[27] G.Alemanni,[23] J.Allaby,[18] A.Aloisio,[30] G.Alverson,[12] M.G.Alviggi,[30] G.Ambrosi,[20] H.Anderhub,[50] V.P.Andreev,[39] T.Angelescu,[13] F.Anselmo,[9] A.Arefiev,[29] T.Azemoon,[3] T.Aziz,[10] P.Bagnaia,[38] L.Baksay,[45] R.C.Ball,[3] S.Banerjee,[10] Sw.Banerjee,[10] K.Banicz,[47] A.Barczyk,[50,ψ] R.Barillère,[18] L.Barone,[38] P.Bartalini,[35] A.Baschirotto,[28] M.Basile,[9] R.Battiston,[35] A.Bay,[23] F.Becattini,[17] U.Becker,[16] F.Behner,[50] J.Berdugo,[27] P.Berges,[16] B.Bertucci,[35] B.L.Betev,[50] S.Bhattacharya,[10] M.Biasini,[18] A.Biland,[50] G.M.Bilei[35] J.J.Blaising,[4] S.C.Blyth,[36] G.J.Bobbink,[2] R.Bock,[1] A.Böhm,[1] L.Boldizsar,[14] B.Borgia,[38] A.Boucham,[4] D.Bourilkov,[50] M.Bourquin,[20] D.Boutigny,[4] S.Braccini,[20] J.G.Branson,[41] V.Brigljevic,[50] I.C.Brock,[36] A.Buffini,[17] A.Buijs,[46] J.D.Burger,[16] W.J.Burger,[20] J.Busenitz,[45] X.D.Cai,[16] M.Campanelli,[50] M.Capell,[16] G.Cara Romeo,[9] G.Carlino,[30] A.M.Cartacci,[17] J.Casaus,[27] G.Castellini,[17] F.Cavallari,[38] N.Cavallo,[30] C.Cecchi,[20] M.Cerrada,[27] F.Cesaroni,[24] M.Chamizo,[27] Y.H.Chang,[52] U.K.Chaturvedi,[19] S.V.Chekanov,[32] M.Chemarin,[26] A.Chen,[52] G.Chen,[7] G.M.Chen,[7] H.F.Chen,[21] H.S.Chen,[7] M.Chen,[16] G.Chiefari,[30] C.Y.Chien,[5] L.Cifarelli,[40] F.Cindolo,[9] C.Civinini,[17] I.Clare,[16] R.Clare,[16] H.O.Cohn,[33] G.Coignet,[4] A.P.Colijn,[2] N.Colino,[27] V.Commichau,[1] S.Costantini,[8] F.Cotorobai,[13] B.de la Cruz,[27] A.Csilling,[14] T.S.Dai,[16] R.D'Alessandro,[17] R.de Asmundis,[30] A.Degré,[4] K.Deiters,[48] P.Denes,[37] F.DeNotaristefani,[38] D.DiBitonto,[45] M.Diemoz,[38] D.van Dierendonck,[2] F.Di Lodovico,[50] C.Dionisi,[38] M.Dittmar,[50] A.Dominguez,[41] A.Doria,[30] I.Dorne,[4] M.T.Dova,[19,♯] E.Drago,[30] D.Duchesneau,[4] P.Duinker,[2] I.Duran,[42] S.Dutta,[10] S.Easo,[35] Yu.Efremenko,[33] H.El Mamouni,[26] A.Engler,[36] F.J.Eppling,[16] F.C.Erné,[2] J.P.Ernenwein,[26] P.Extermann,[20] M.Fabre,[48] R.Faccini,[38] S.Falciano,[38] A.Favara,[17] J.Fay,[26] O.Fedin,[39] M.Felcini,[50] B.Fenyi,[45] T.Ferguson,[36] F.Ferroni,[38] H.Fesefeldt,[1] E.Fiandrini,[35] J.H.Field,[20] F.Filthaut,[36] P.H.Fisher,[16] I.Fisk,[41] G.Forconi,[16] L.Fredj,[20] K.Freudenreich,[50] C.Furetta,[28] Yu.Galaktionov,[29,16] S.N.Ganguli,[10] P.Garcia-Abia,[49] S.S.Gau,[12] S.Gentile,[38] J.Gerald,[5] N.Gheordanescu,[13] S.Giagu,[38] S.Goldfarb,[23] J.Goldstein,[11] Z.F.Gong,[21] A.Gougas,[5] G.Gratta,[34] M.W.Gruenewald,[8] V.K.Gupta,[37] A.Gurtu,[10] L.J.Gutay,[47] B.Hartmann,[1] A.Hasan,[31] D.Hatzifotiadou,[9] T.Hebbeker,[8] A.Hervé,[18] W.C.van Hoek,[32] H.Hofer,[50] S.J.Hong,[44] H.Hoorani,[36] S.R.Hou,[52] G.Hu,[5] V.Innocente,[18] H.Janssen,[4] K.Jenkes,[1] B.N.Jin,[7] L.W.Jones,[3] P.de Jong,[18] I.Josa-Mutuberria,[27] A.Kasser,[23] R.A.Khan,[19] D.Kamrad,[49] Yu.Kamyshkov,[33] J.S.Kapustinsky,[25] Y.Karyotakis,[4] M.Kaur,[19,◇] M.N.Kienzle-Focacci,[20] D.Kim,[38] D.H.Kim,[44] J.K.Kim,[44] S.C.Kim,[44] Y.G.Kim,[44] W.W.Kinnison,[25] A.Kirkby,[34] D.Kirkby,[34] J.Kirkby,[18] D.Kiss,[14] W.Kittel,[32] A.Klimentov,[16,29] A.C.König,[32] A.Kopp,[49] I.Korolko,[29] V.Koutsenko,[16,29] R.W.Kraemer,[36] W.Krenz,[1] A.Kunin,[16,29] P.Ladron de Guevara,[27] G.Landi,[17] C.Lapoint,[16] K.Lassila-Perini,[50] P.Laurikainen,[22] M.Lebeau,[18] A.Lebedev,[16] P.Lebrun,[26] P.Lecomte,[50] P.Lecoq,[18] P.Le Coultre,[50] C.Leggett,[3] J.M.Le Goff,[18] R.Leiste,[49] E.Leonardi,[38] P.Levtchenko,[39] C.Li,[21] C.H.Lin,[52] W.T.Lin,[52] F.L.Linde,[2,18] L.Lista,[30] Z.A.Liu,[7] W.Lohmann,[49] E.Longo,[38] W.Lu,[34] Y.S.Lu,[7] K.Lübelsmeyer,[1] C.Luci,[38] D.Luckey,[16] L.Luminari,[38] W.Lustermann,[48] W.G.Ma,[21] M.Maity,[10] G.Majumder,[10] L.Malgeri,[38] A.Malinin,[29] C.Maña,[27] D.Mangeol,[32] S.Mangla,[10] P.Marchesini,[50] A.Marin,[11] J.P.Martin,[26] F.Marzano,[38] G.G.G.Massaro,[2] D.McNally,[18] S.Mele,[30] L.Merola,[30] M.Meschini,[17] W.J.Metzger,[32] M.von der Mey,[1] Y.Mi,[23] A.Mihul,[13] A.J.W.van Mil,[32] G.Mirabelli,[38] J.Mnich,[18] P.Molnar,[8] B.Monteleoni,[17] R.Moore,[3] S.Morganti,[38] T.Moulik,[10] R.Mount,[34] S.Müller,[1] F.Muheim,[20] A.J.M.Muijs,[2] S.Nahn,[16] M.Napolitano,[30] F.Nessi-Tedaldi,[50] H.Newman,[34] T.Niessen,[1] A.Nippe,[1] A.Nisati,[38] H.Nowak,[49] Y.D.Oh,[44] H.Opitz,[1] G.Organtini,[38] R.Ostonen,[22] C.Palomares,[27] D.Pandoulas,[1] S.Paoletti,[38] P.Paolucci,[30] H.K.Park,[36] I.H.Park,[44] G.Pascale,[38] G.Passaleva,[17] S.Patricelli,[30] T.Paul,[12] M.Pauluzzi,[35] C.Paus,[1] F.Pauss,[50] D.Peach,[18] Y.J.Pei,[1] S.Pensotti,[28] D.Perret-Gallix,[4] B.Petersen,[32] S.Petrak,[8] A.Pevsner,[5] D.Piccolo,[30] M.Pieri,[17] J.C.Pinto,[36] P.A.Piroué,[37] E.Pistolesi,[28] V.Plyaskin,[29] M.Pohl,[50] V.Pojidaev,[29,17] H.Postema,[16] N.Produit,[20] D.Prokofiev,[39] G.Rahal-Callot,[50] N.Raja,[10] P.G.Rancoita,[28] M.Rattaggi,[28] G.Raven,[41] P.Razis,[31] K.Read,[33] D.Ren,[50] M.Rescigno,[38] S.Reucroft,[12] T.van Rhee,[46] S.Riemann,[49] K.Riles,[3] O.Rind,[3] A.Robohm,[50] J.Rodin,[16] B.P.Roe,[3] L.Romero,[27] S.Rosier-Lees,[4] Ph.Rosselet,[23] W.van Rossum,[46] S.Roth,[1] J.A.Rubio,[18] D.Ruschmeier,[8] H.Rykaczewski,[50] J.Salicio,[18] E.Sanchez,[27] M.P.Sanders,[32] M.E.Sarakinos,[22] S.Sarkar,[10] M.Sassowsky,[1] G.Sauvage,[4] C.Schäfer,[1] V.Schegelsky,[39] S.Schmidt-Kaerst,[1] D.Schmitz,[1] P.Schmitz,[1] M.Schneegans,[4] N.Scholz,[50] H.Schopper,[51] D.J.Schotanus,[32] J.Schwenke,[1] G.Schwering,[1] C.Sciacca,[30] D.Sciarrino,[20] L.Servoli,[35] S.Shevchenko,[34] N.Shivarov,[43] V.Shoutko,[29] J.Shukla,[25] E.Shumilov,[29] A.Shvorob,[34] T.Siedenburg,[1] D.Son,[44] A.Sopczak,[49] V.Soulimov,[30] B.Smith,[16] P.Spillantini,[17] M.Steuer,[16] D.P.Stickland,[37] H.Stone,[37] B.Stoyanov,[43] A.Straessner,[1] K.Strauch,[15] K.Sudhakar,[10] G.Sultanov,[19] L.Z.Sun,[21] G.F.Susinno,[20] H.Suter,[50] J.D.Swain,[19] X.W.Tang,[7] L.Tauscher,[6] L.Taylor,[12] Samuel C.C.Ting,[16] S.M.Ting,[16] M.Tonutti,[1] S.C.Tonwar,[10] J.Tóth,[14] C.Tully,[37] H.Tuchscherer,[45] K.L.Tung,[7] Y.Uchida,[16] J.Ulbricht,[50] U.Uwer,[18] E.Valente,[38] R.T.Van de Walle,[32] G.Vesztergombi,[14] I.Vetlitsky,[29] G.Viertel,[50] M.Vivargent,[4] R.Völkert,[49] H.Vogel,[36] H.Vogt,[49] I.Vorobiev,[29] A.A.Vorobyov,[39] A.Vorvolakos,[31] M.Wadhwa,[6] W.Wallraff,[1] J.C.Wang,[16] X.L.Wang,[21] Z.M.Wang,[21] A.Weber,[1] F.Wittgenstein,[18] S.X.Wu,[19] S.Wynhoff,[1] J.Xu,[11] Z.Z.Xu,[21] B.Z.Yang,[21] C.G.Yang,[7] X.Y.Yao,[7] J.B.Ye,[21] S.C.Yeh,[52] J.M.You,[36] An.Zalite,[39] Yu.Zalite,[39] P.Zemp,[50] Y.Zeng,[1] Z.Zhang,[7] Z.P.Zhang,[21] B.Zhou,[11] Y.Zhou,[3] G.Y.Zhu,[7] R.Y.Zhu,[34] A.Zichichi,[9,18,19] F.Ziegler.[49]

1 I. Physikalisches Institut, RWTH, D-52056 Aachen, FRG[§]
III. Physikalisches Institut, RWTH, D-52056 Aachen, FRG[§]
2 National Institute for High Energy Physics, NIKHEF, and University of Amsterdam, NL-1009 DB Amsterdam, The Netherlands
3 University of Michigan, Ann Arbor, MI 48109, USA
4 Laboratoire d'Annecy-le-Vieux de Physique des Particules, LAPP,IN2P3-CNRS, BP 110, F-74941 Annecy-le-Vieux CEDEX, France
5 Johns Hopkins University, Baltimore, MD 21218, USA
6 Institute of Physics, University of Basel, CH-4056 Basel, Switzerland
7 Institute of High Energy Physics, IHEP, 100039 Beijing, China[△]
8 Humboldt University, D-10099 Berlin, FRG[§]
9 University of Bologna and INFN-Sezione di Bologna, I-40126 Bologna, Italy
10 Tata Institute of Fundamental Research, Bombay 400 005, India
11 Boston University, Boston, MA 02215, USA
12 Northeastern University, Boston, MA 02115, USA
13 Institute of Atomic Physics and University of Bucharest, R-76900 Bucharest, Romania
14 Central Research Institute for Physics of the Hungarian Academy of Sciences, H-1525 Budapest 114, Hungary[‡]
15 Harvard University, Cambridge, MA 02139, USA
16 Massachusetts Institute of Technology, Cambridge, MA 02139, USA
17 INFN Sezione di Firenze and University of Florence, I-50125 Florence, Italy
18 European Laboratory for Particle Physics, CERN, CH-1211 Geneva 23, Switzerland
19 World Laboratory, FBLJA Project, CH-1211 Geneva 23, Switzerland
20 University of Geneva, CH-1211 Geneva 4, Switzerland
21 Chinese University of Science and Technology, USTC, Hefei, Anhui 230 029, China[△]
22 SEFT, Research Institute for High Energy Physics, P.O. Box 9, SF-00014 Helsinki, Finland
23 University of Lausanne, CH-1015 Lausanne, Switzerland
24 INFN-Sezione di Lecce and Universitá Degli Studi di Lecce, I-73100 Lecce, Italy
25 Los Alamos National Laboratory, Los Alamos, NM 87544, USA
26 Institut de Physique Nucléaire de Lyon, IN2P3-CNRS,Université Claude Bernard, F-69622 Villeurbanne, France
27 Centro de Investigaciones Energeticas, Medioambientales y Tecnologicas, CIEMAT, E-28040 Madrid, Spain[♭]
28 INFN-Sezione di Milano, I-20133 Milan, Italy
29 Institute of Theoretical and Experimental Physics, ITEP, Moscow, Russia
30 INFN-Sezione di Napoli and University of Naples, I-80125 Naples, Italy
31 Department of Natural Sciences, University of Cyprus, Nicosia, Cyprus
32 University of Nijmegen and NIKHEF, NL-6525 ED Nijmegen, The Netherlands
33 Oak Ridge National Laboratory, Oak Ridge, TN 37831, USA
34 California Institute of Technology, Pasadena, CA 91125, USA
35 INFN-Sezione di Perugia and Universitá Degli Studi di Perugia, I-06100 Perugia, Italy
36 Carnegie Mellon University, Pittsburgh, PA 15213, USA
37 Princeton University, Princeton, NJ 08544, USA
38 INFN-Sezione di Roma and University of Rome, "La Sapienza", I-00185 Rome, Italy
39 Nuclear Physics Institute, St. Petersburg, Russia
40 University and INFN, Salerno, I-84100 Salerno, Italy
41 University of California, San Diego, CA 92093, USA
42 Dept. de Fisica de Particulas Elementales, Univ. de Santiago, E-15706 Santiago de Compostela, Spain
43 Bulgarian Academy of Sciences, Central Lab. of Mechatronics and Instrumentation, BU-1113 Sofia, Bulgaria
44 Center for High Energy Physics, Korea Adv. Inst. of Sciences and Technology, 305-701 Taejon, Republic of Korea
45 University of Alabama, Tuscaloosa, AL 35486, USA
46 Utrecht University and NIKHEF, NL-3584 CB Utrecht, The Netherlands
47 Purdue University, West Lafayette, IN 47907, USA
48 Paul Scherrer Institut, PSI, CH-5232 Villigen, Switzerland
49 DESY-Institut für Hochenergiephysik, D-15738 Zeuthen, FRG
50 Eidgenössische Technische Hochschule, ETH Zürich, CH-8093 Zürich, Switzerland
51 University of Hamburg, D-22761 Hamburg, FRG
52 High Energy Physics Group, Taiwan, China

§ Supported by the German Bundesministerium für Bildung, Wissenschaft, Forschung und Technologie
‡ Supported by the Hungarian OTKA fund under contract numbers T14459 and T24011.
♭ Supported also by the Comisión Interministerial de Ciencia y Tecnología
♯ Also supported by CONICET and Universidad Nacional de La Plata, CC 67, 1900 La Plata, Argentina
♢ Also supported by Panjab University, Chandigarh-160014, India
△ Supported by the National Natural Science Foundation of China.

Particle Type	Efficiency (%)	Purity (%)
e	60	94
μ	51	94
π	65	81

Table 1: The efficiency and purity of the neural network for three different particles types.

Background channel	Expected in $e^+e^-e^+e^-$ (%)	Expected in $e^+e^-\mu^+\mu^-$ (%)	Expected in $e^+e^-\tau^+\tau^-$ (%)
$Z \to e^+e^-$	0.16 ± 0.02	0.11 ± 0.03	-
$Z \to \mu^+\mu^-$	0.006 ± 0.004	0.08 ± 0.03	-
$Z \to \tau^+\tau^-$	0.12 ± 0.02	0.11 ± 0.03	1.0 ± 0.5
$e^+e^- \to e^+e^- f_2$	0.34 ± 0.03	3.6 ± 0.02	-
$e^+e^- \to e^+e^-e^+e^-$	-	-	3.5 ± 3.5
$e^+e^- \to e^+e^-\mu^+\mu^-$	0.85 ± 0.06	-	4.0 ± 4.0
$e^+e^- \to e^+e^-\eta'$	-	-	0.4 ± 0.4
Total	1.5 ± 0.07	3.9 ± 0.2	8.9 ± 5.4

Table 2: Background fractions for the electron, muon and tau pair samples.

Channel	observed events	expected events	obs. / expect.
$e^+e^-e^+e^-$	$30584 \pm 174 \pm 532$	30890 ± 278	0.99 ± 0.02
$e^+e^-\mu^+\mu^-$	$11875 \pm 108 \pm 230$	11764 ± 187	1.01 ± 0.02
$e^+e^-\tau^+\tau^-$ ($e\mu$)	$140 \pm 12 \pm 17$	135 ± 9	1.04 ± 0.17
$e^+e^-\tau^+\tau^-$ ($l\pi^\pm\pi^0$)	$93 \pm 10 \pm 3$	99 ± 7	0.94 ± 0.15

Table 3: Observed and expected numbers of events in the different dilepton channels. The numbers of observed events have the background subtracted.

Source	$e\mu$ Channel	$l\pi^\pm\pi^0$ Channel
Trigger	0.02	0.02
$\Delta\epsilon$	0.07	0.10
Background	0.11	0.01
NN	0.03	0.03
MC Statistics	0.06	0.07
Total	0.15	0.13

Table 4: Details of the systematic errors on total cross section for $e^+e^- \to e^+e^-\tau^+\tau^-$.

References

[1] PLUTO Collab., Ch. Berger *et al.*, Z. Phys. **C 27** (1985) 249;
JADE Collab., W. Bartel *et al.*, Z. Phys. **C 30** (1986) 545;
MARK-J Collab., B. Adeva *et al.*, Phys. Rev. **D 38** (1988) 2665;
CELLO Collab., H.J. Behrend *et al.*, Z. Phys. **C 43** (1989) 1;
AMY Collab., Y.H. Ho *et al.*, Phys. Lett. **B 244** (1990) 573.

[2] L3 Collab., B. Adeva *et al.*, Nucl. Inst. Meth. **A 289** (1990) 35;
L3 Collab., O. Adriani *et al.*, Physics Reports **236** (1993) 1.

[3] OPAL Collab., R. Akers *et al.*, Z. Phys. **C 60** (1993) 593.

[4] P. Bene *et al.*, Nucl. Inst. Meth. **A 306** (1991) 150.

[5] F.A. Berends, P.H. Daverveldt and R. Kleiss, Comp. Phys. Com. **40** (1986) 285.

[6] F. Linde, "Workshop on detector and event simulation in high energy physics-Monte Carlo", eds. K. Bos and B. van Eijl, Amsterdam, 1991.

[7] The L3 detector simulation is based on GEANT Version 3.15.
See R. Brun *et al.*, "GEANT 3", CERN DD/EE/84-1 (Revised), September 1987.
The GHEISHA program (H. Fesefeldt, RWTH Aachen Report PITHA 85/02 (1985)) is used to simulate hadronic interactions.

[8] M. Campanelli, "Evidence of $e^+e^- \to e^+e^-\tau^+\tau^-$ production in leptonic and semileptonic decay channels",L3 Internal Note No. 1857, 1995, unpublished.

[9] H. Hoorani, "The level-1 charged particle trigger of L3 detector and the study of two-photon production in e^+e^- and $\mu^+\mu^-$ pairs in untagged events",Ph.D. Thesis, Université de Genève, Genève, 1996.

[10] R.M. Barnett *et al.*, Particle Data Group, Phys. Rev. **D 54** (1996) 1.

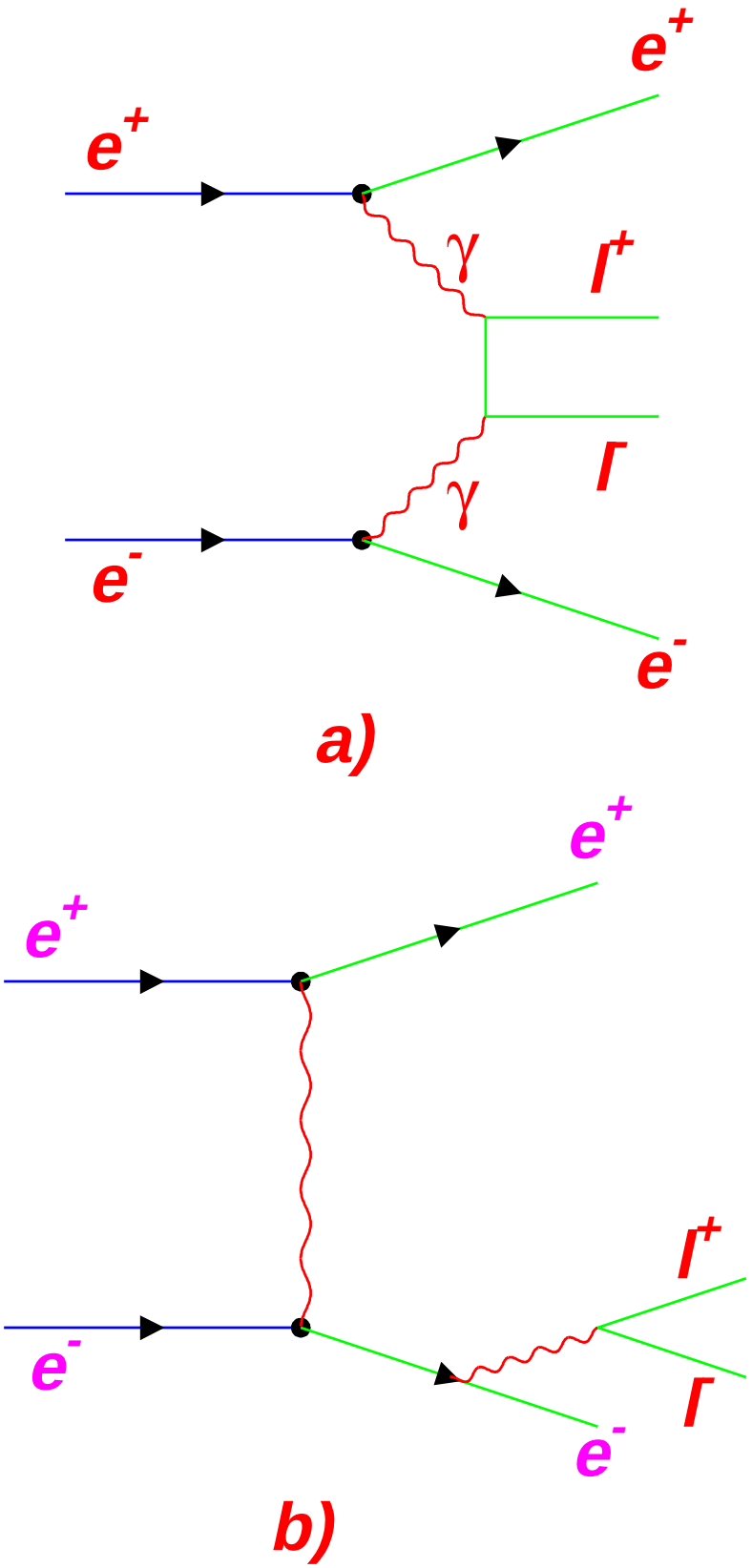

Figure 1: Typical diagrams of order α^4 contributing to the lepton-pair production in e^+e^- collisions: a) Multiperipheral, b) bremsstrahlung.

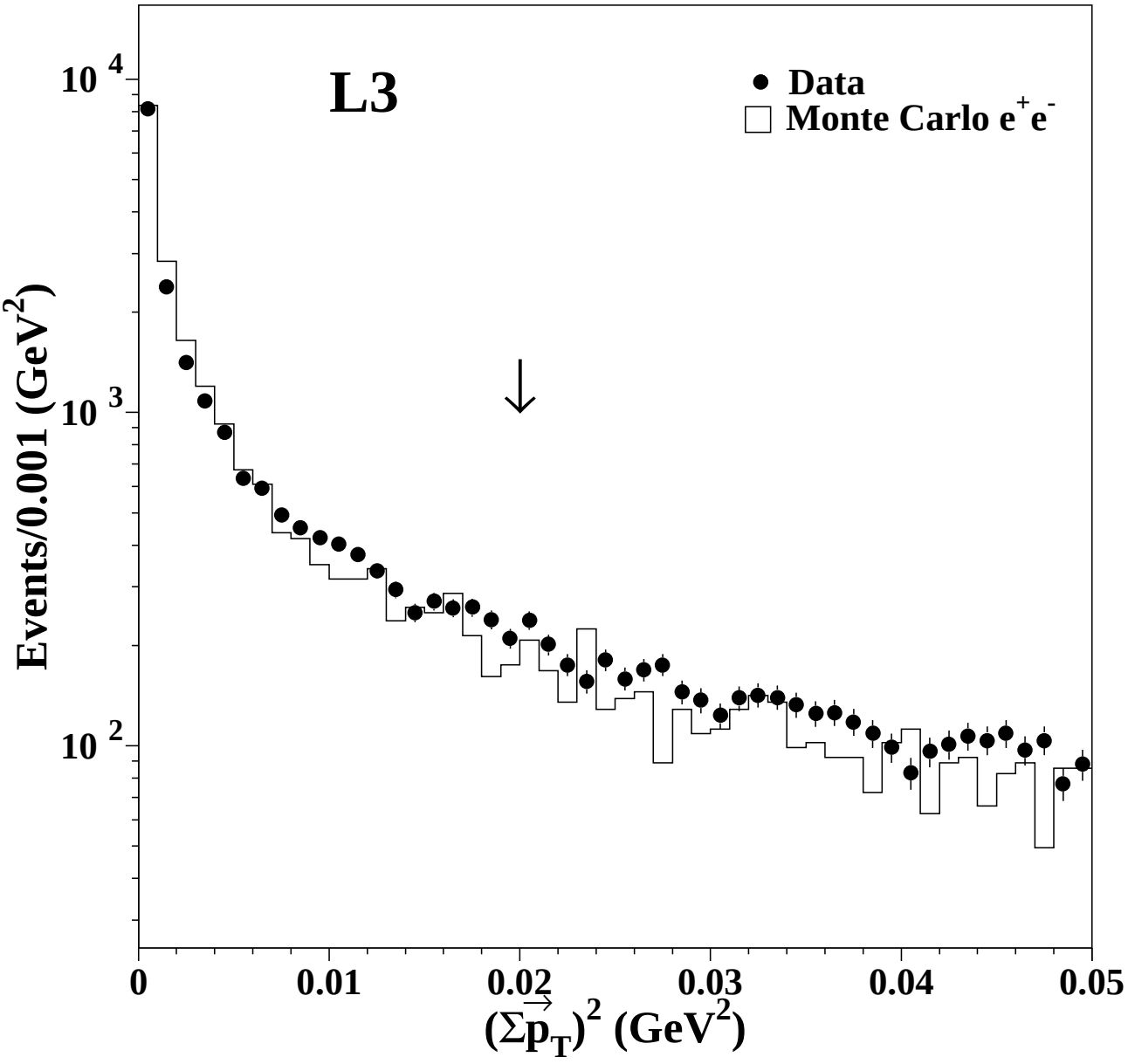

Figure 2: The square of the total transverse momentum of the observed lepton pair for the channel $e^+e^- \to e^+e^-e^+e^-$ with all selection cuts applied except the cut on the variable shown.

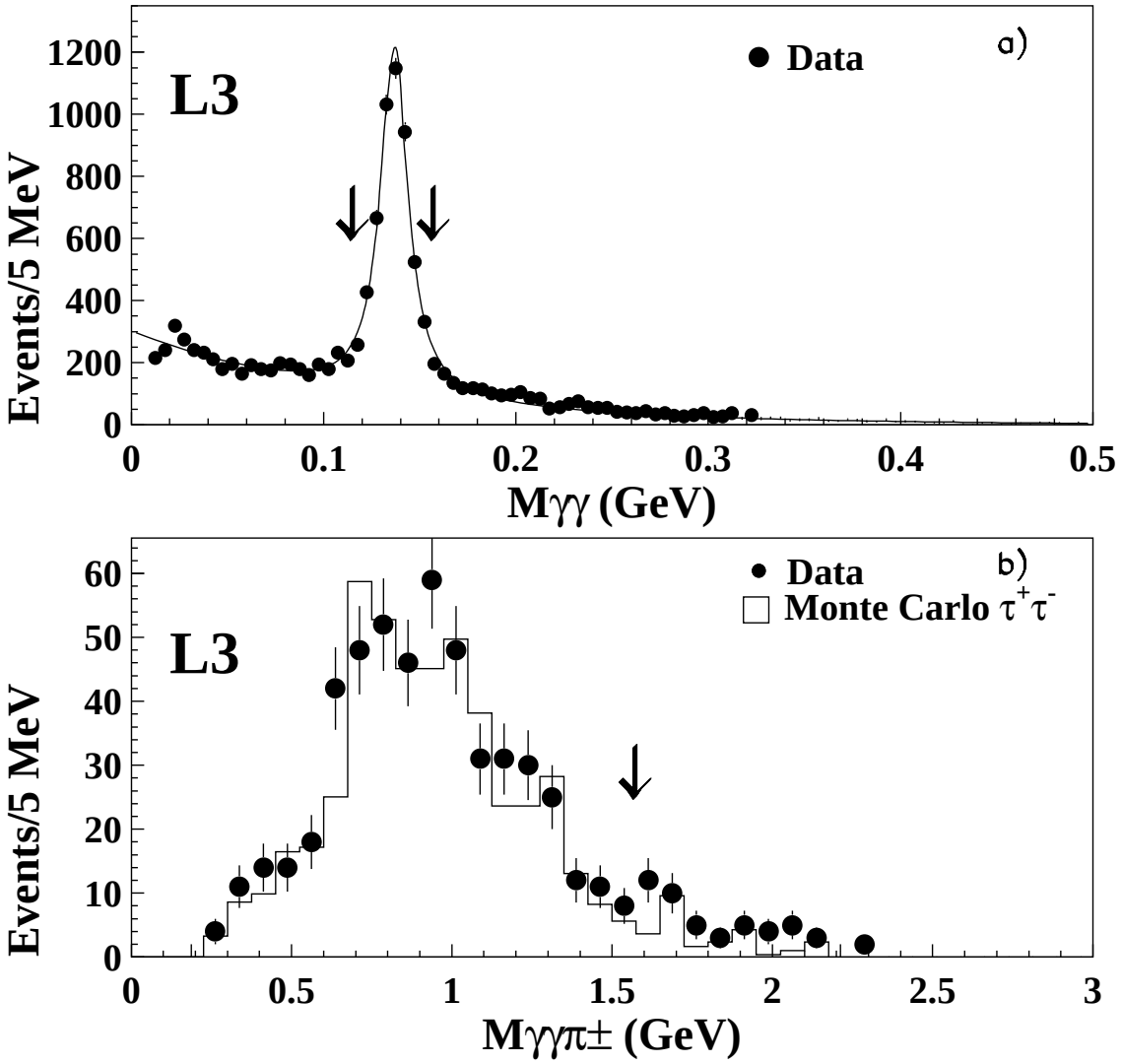

Figure 3: a) The invariant mass distribution of two electromagnetic clusters not associated with charged tracks. The peak value of the fitted Gaussian is at 135.2 ± 0.2 MeV. b) The invariant mass distribution of the $\pi^{\pm}\gamma\gamma$ system both for data and for signal events in Monte Carlo.

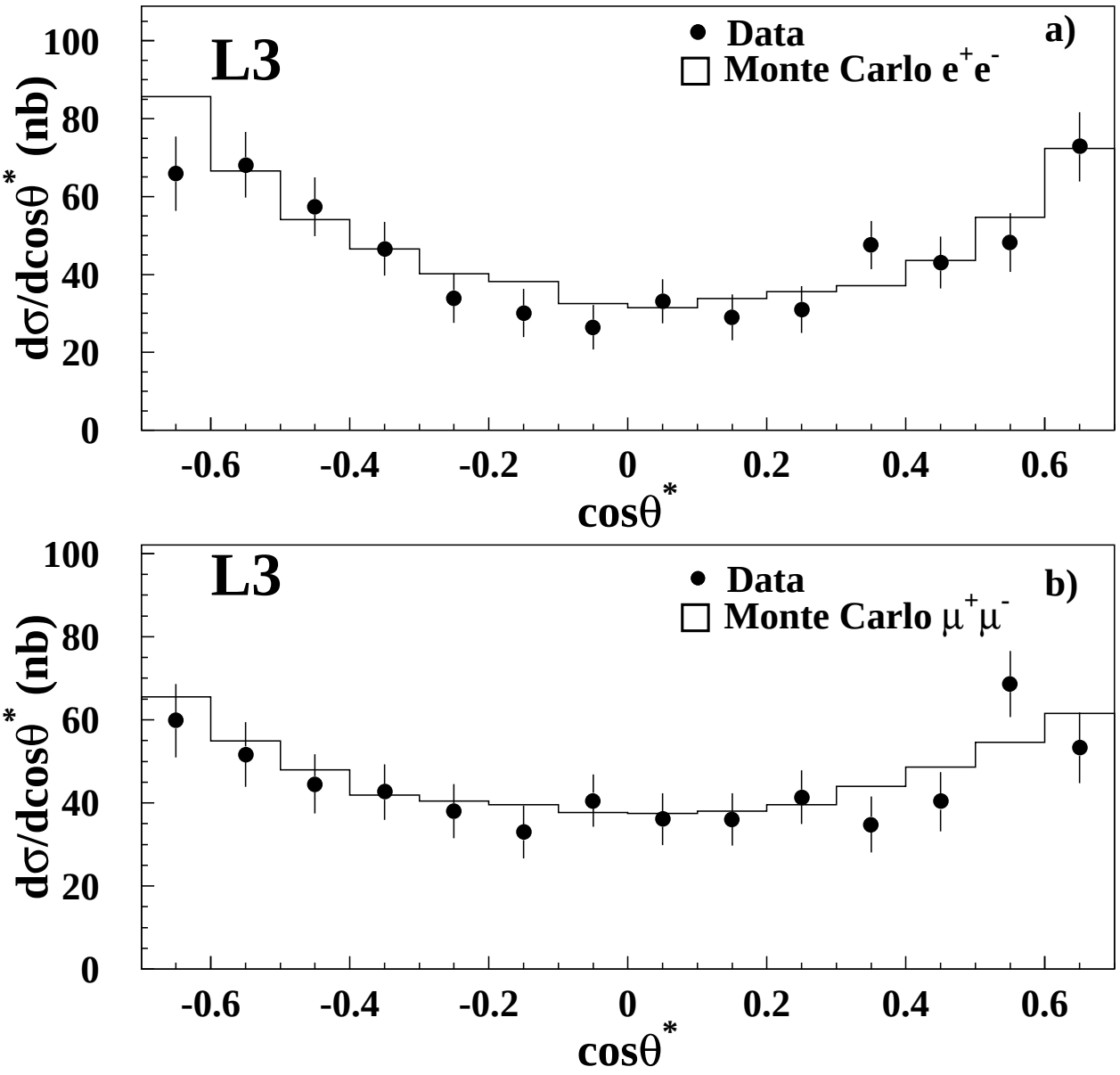

Figure 4: Comparison of the measured and expected differential cross sections as a function of cos θ^*, for a) electron pairs , b) muon pairs.

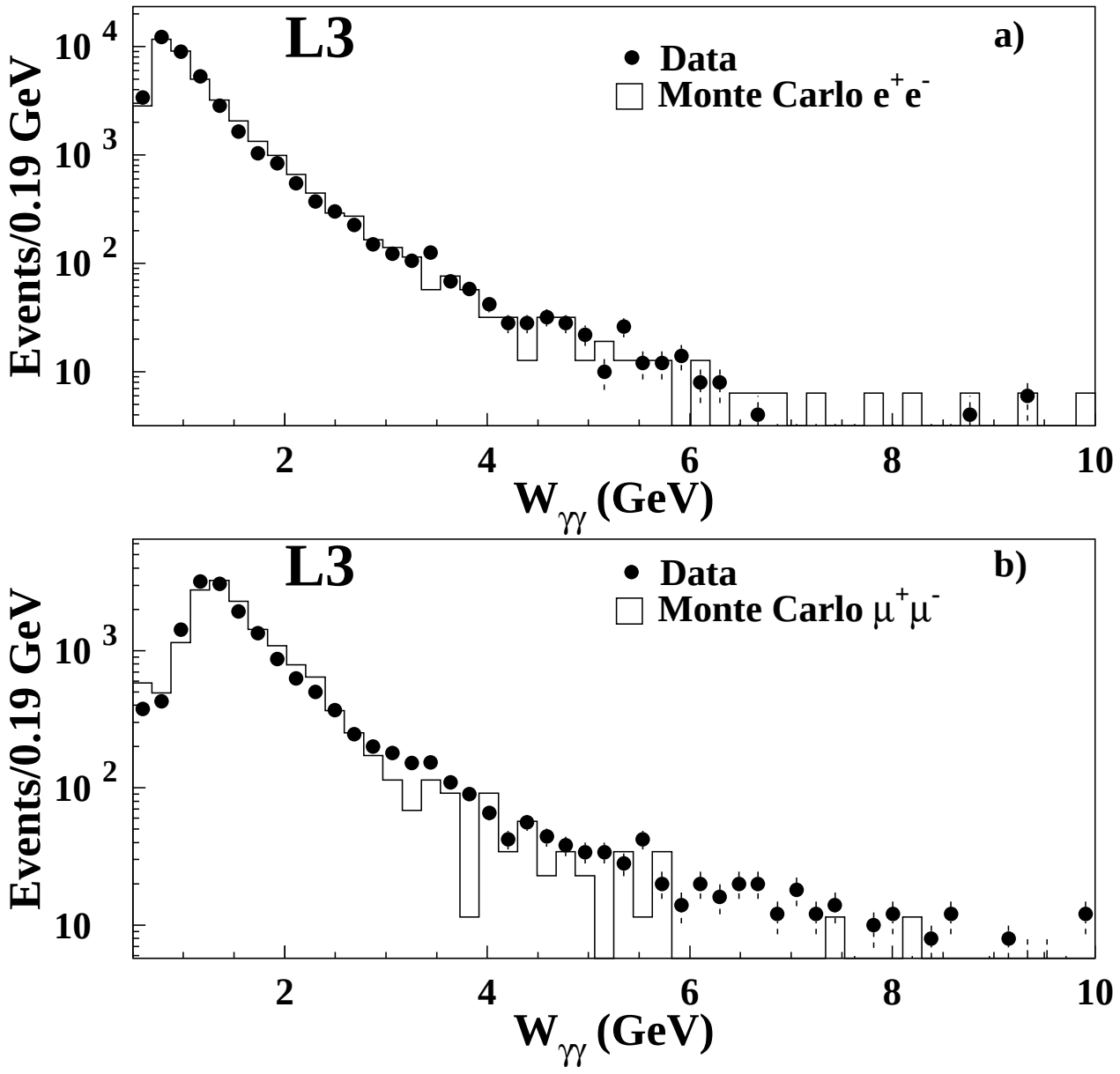

Figure 5: The invariant mass distribution for events where a) one track is identified as an electron and b) one track is identified as a muon. For both channels background is subtracted bin-by-bin. The data are the points with error bars and the Monte Carlo prediction is the histogram.

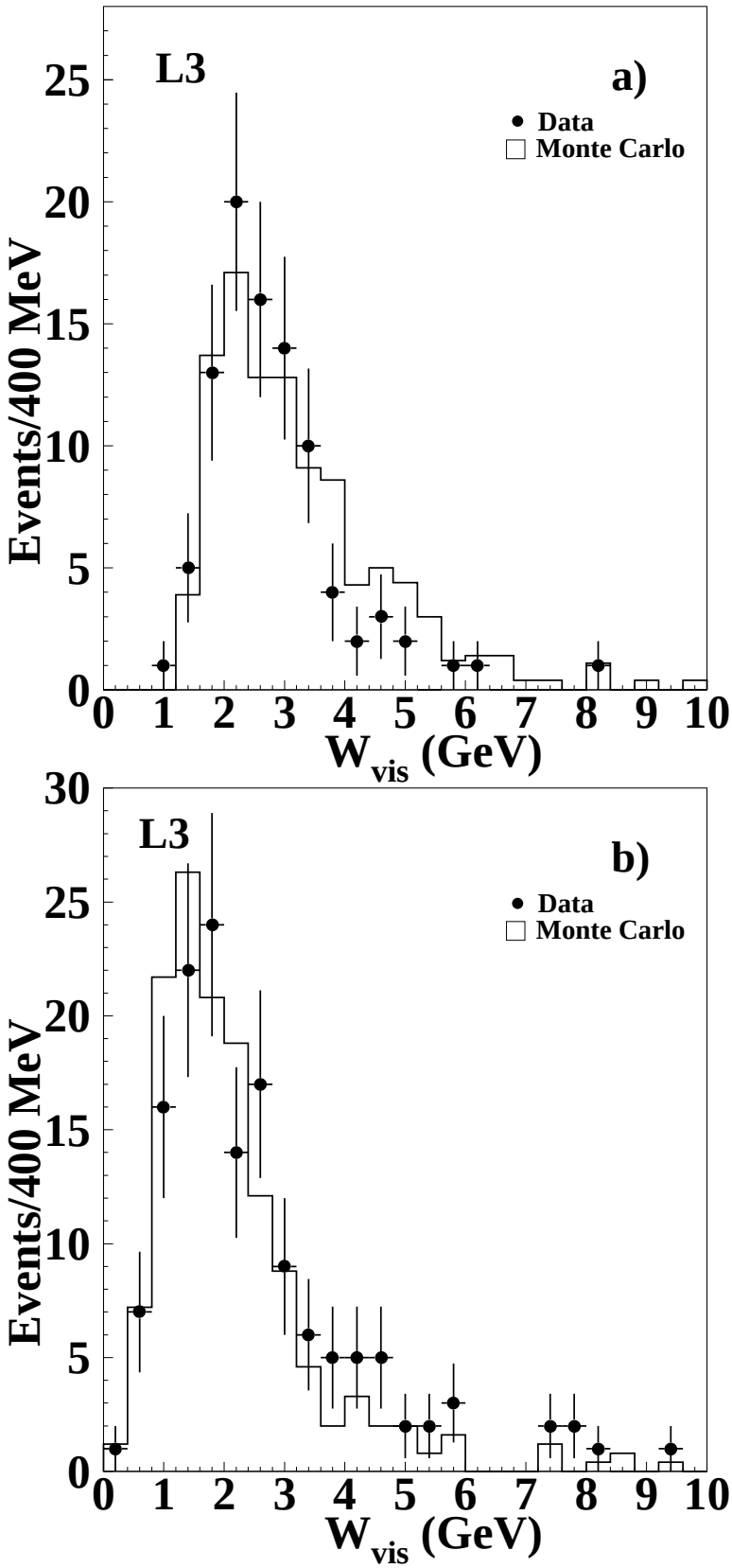

Figure 6: The invariant mass distribution of all the observed particles for selected τ events is shown for the data and the Monte Carlo for the τ decay channel a) $l^{\pm}\pi^{\pm}\pi^{0}$ and b) $e^{\pm}\mu^{\pm}$. For both cases the background has been subtracted.